Optical and Quantum Electronics (2006) 38:445–465
DOI 10.1007/s11082-006-0042-5
© Springer 2006

Polarization and transverse mode behaviour of VCSELs under optical injection

M. S. TORRE[1], A. VALLE[2,*] AND L. PESQUERA[2]
[1]*Instituto de Física Arroyo Seco, Universidad Nacional del Centro de la Provincia de Buenos Aires (UNCPBA), Pinto 399 (7000), Tandil, Argentina*
[2]*Instituto de Física de Cantabria, CSIC-Universidad de Cantabria, Avda. Los Castros s/n, E-39005, Santander, Spain*
*(*author for correspondence: E-mail: valle@ifca.unican.es)*

Received 21 June 2005; accepted 26 January 2006

Abstract. A theoretical analysis of the polarization and transverse modes of Vertical-cavity Surface-emitting lasers with external optical injection is performed. We show that, for single-mode operation, weak injection of linearly polarized light can lead to stable output power in the injected polarization. We also show that, for multitransverse mode operation, weak injection of linearly-polarized light can lead to stable emission of the fundamental transverse mode in the injected polarization over wide current ranges. The previous selection can occur when the transverse modes have parallel or orthogonal polarizations.

Key words: transverse modes, vertical-cavity lasers, polarization, semiconductor lasers, injection

1. Introduction

Vertical-cavity surface-emitting lasers (VCSELs) are semiconductor lasers with a unique geometry that results in significant advantages over their edge-emitting counterparts, including low threshold current, low cost, circular output beam and easy fabrication in two-dimensional arrays. Although VCSELs are intrinsically single-longitudinal mode devices, emission in multiple transverse and polarization modes is usually found (Chang-Hasnain *et al.* 1991). While emission in several transverse modes is usually attributed to Spatial Hole Burning (SHB) effects (Chang-Hasnain *et al.* 1991; Vakhshoori *et al.* 1993; Valle *et al.* 1995), several physical mechanisms have been proposed to explain the polarization behaviour of these devices (Choquette *et al.* 1995; San Miguel *et al.* 1995; Valle *et al.* 1996; Panajotov *et al.* 1998; Ryvkin *et al.* 1999). Joint consideration of previous physical mechanisms (Martin-Regalado *et al.* 1997a; Valle *et al.* 1997; Balle *et al.* 1999, Mulet and Balle 2003) has helped to better understand the polarization behaviour of multitransverse mode VCSELs.

Injection locking of semiconductor lasers has been a subject of interest for many years (Lang 1982; van Tartwijk and Lenstra 1995). Applications

include laser spectral narrowing, suppression of laser noise, reduction of frequency chirp under modulation and improving the laser intrinsic frequency response. The VCSELs are also attractive for use in injection locking because of its compactness, low power consumption and circular output beam (Onishi *et al.* 2004a). Experimental studies of injection locking in VCSELs show a dependence on the power of the injected signal and frequency detuning that is similar to the case of edge-emitting lasers (Li *et al.* 1996). Further experimental works have shown the possibility of using injection in VCSELs to perform several optical signal-processing functions (Onishi *et al.* 2004b), to significatively increase the resonance frequency in VCSELs (Chang *et al.* 2003), to achieve transverse mode selection (Hong *et al.* 2002) and polarization control (Bandyopadhyay *et al.* 2003). Optical injection can also be used to obtain rich non-linear dynamics in VCSELs (Law *et al.* 1997; Hong *et al.* 2003). The use of optical injection complements another strategies to obtain chaotic behaviour in VCSELs like the use of current modulation (Valle *et al.* 2002; Sciamanna *et al.* 2003a) or optical feedback (Yu *et al.* 2001), finding applications in optical chaotic communication systems.

Theoretical modelling of VCSELs operating under injection conditions has been performed for a linearly polarized single transverse mode (Chang *et al.* 2003). The addition of the polarization degree of freedom has also been theoretically considered (Sciamanna *et al.* 2003b). Consideration of spatial effects has permitted the theoretical analysis of the effect of optical injection on the multiple transverse mode emission of VCSELs (Law *et al.* 1997; Torre *et al.* 2004). These works have focused on the possibility of selecting a transverse mode by appropriate light injection. Results showed that a two-mode VCSEL can be forced to operate in a single transverse mode if the linear polarization of both transverse modes is orthogonal (Law *et al.* 1997; Torre *et al.* 2004) while the laser does not turn into a single-mode laser if both transverse modes have parallel polarizations (Torre *et al.* 2004). That is precisely the situation that has been found in recent experimental work (Hong *et al.* 2002). However there is also experimental work that shows that single transverse mode operation can be obtained by injection locking when the modes have parallel polarizations (Onishi *et al.* 2004a). A certain variety of experimental results is then found. We also note that the previous theoretical models (Law *et al.* 1997; Torre *et al.* 2004) do not take into account any of the physical mechanisms (Choquette *et al.* 1995; San Miguel *et al.* 1995; Valle *et al.* 1996; Panajotov *et al.* 1998; Ryvkin *et al.* 1999) that can determine the VCSEL polarization. Both previous facts have motivated us to study the problem of injection locking in multitransverse mode VCSELs by considering the polarization evolution in a more consistent way. We have then considered a model (Martin-Regalado *et al.* 1997a; Valle *et al.* 1998a) that incorporates

two of the polarization defining mechanisms. The first mechanism is associated to the combined effect of VCSEL anisotropies, alpha factor and spin flip relaxation processes within a theoretical framework, known as the SFM model, that includes the quantum states of the energy levels involved in the lasing process (San Miguel *et al.* 1995). The second mechanism (Valle *et al.* 1996) is related to the effect of having different electrical field profiles for each linear polarization due to the birefringence of the device:the different spatial overlap of the electrical field profile for each polarization with the carrier density profile leads to different modal gains for each polarization producing then polarization selection. The model also takes into account the spatial dependence of the system to properly describe the SHB effects that lead to multiple transverse mode emission.

In this work we will use the joint model (Martin-Regalado *et al.* 1997a; Valle *et al.* 1998a) to show that weak injection of linearly-polarized light in multimode VCSELs can lead to stable emission of the fundamental transverse mode in the injected polarization over wide current ranges. This selection can occur when the transverse modes have parallel or orthogonal polarizations. We will also discuss the detuning range over, which the previous selection of the fundamental mode is effective. The paper is organised as follows. In Section 2 the theoretical model is presented. Section 3 is devoted to the study of optical injection in single transverse mode VCSELs. In Section 4 we focus on the optical injection effects in multitransverse mode VCSELs. Finally in Section 5 a discussion and summary are presented.

2. Model

We consider cilindrically symmetric weak index-guided devices. Subscripts x and y will be used to denote the polarization direction. Birefringency is taken into account by assuming that the core refractive index in the x-direction, n_{core}, x, is larger than in the y-direction, $n_{\text{core},y}$-hence the x polarised mode emission frequency is lower than that of the y polarised mode-, while the cladding refractive index, n_{cladd}, is the same in both directions. We will consider small index steps $\Delta n = n_{\text{core},y} - n_{\text{cladd}}$($n_{\text{core},y}$ and n_{cladd} are taken as 3.5 and 3.495, respectively). Then the appropriate modes are the LP_{mn} modes. Here we treat the case of VCSELs that can operate in the fundamental (LP_{01}) and in the first-order (LP_{11}) transverse modes because these modes are the only ones supported by the assumed weak guide. Subscripts 0,1 will be used to denote the LP_{01} and LP_{11} modes, respectively. In the basis of the linearly polarised modes and considering the radial symmetry of the cavity the optical field can be written as:

$$\vec{E}(r,t) = [(E_{0x}(t)\psi_{0x}(r) + E_{1x}(t)\psi_{1x}(r))\,\vec{x} + \left(E_{0y}(t)\psi_{0y}(r) + E_{1y}(t)\psi_{1y}(r)\right)\vec{y}]\,\mathrm{e}^{ik\alpha t} + cc, \tag{1}$$

where ψ_{0j} and ψ_{1j} are the modal profiles of the LP_{01} and LP_{11} modes, respectively, obtained by solving the Helmholtz equation (Valle *et al.* 1996); E_{0j} and E_{1j} are the modal amplitudes of these modes, the subindex j stands for the linear polarization state of the given mode, k is the field decay rate and α is the alpha factor. The model is then based on an expansion of the electrical field in the modal profiles determined by the effective waveguide structure. This model based on modal expansion has been compared with a full spatiotemporal model (Mulet and Balle 2003). The two descriptions agree when the effective index step is greater than the contribution due to the carrier-induced refractive index. This is the case for the index steps that we use in this work (Mulet and Balle 2003). Hence, the equations describing the polarization and transverse mode behaviour of the VCSEL with an injected optical field, written appropriately in the cylindrical basis, read (Martin-Regalado *et al.* 1997a; Valle *et al.* 1998a):

$$\begin{aligned}
\dot{E}_{0x} &= k(1+i\alpha)\left(E_{0x}(g_{0x}-1) + iE_{0y}g_{0xy}\right) - (\gamma_{\mathrm{a}} + i\gamma_{\mathrm{p0}})E_{0x} + \frac{k_{0x}}{\tau_{\mathrm{in}}}\mathrm{e}^{i\Delta\omega t} \\
&\quad + \sqrt{\frac{\beta}{2}}\left(\sqrt{\bar{N}+\bar{n}}\,\xi_{0+}(t) + \sqrt{\bar{N}-\bar{n}}\,\xi_{0-}(t)\right) \\
\dot{E}_{0y} &= k(1+i\alpha)\left(E_{0y}(g_{0y}-1) - iE_{0x}g_{0yx}\right) + (\gamma_{\mathrm{a}} + i\gamma_{\mathrm{p0}})E_{0y} + \frac{k_{0y}}{\tau_{\mathrm{in}}}\mathrm{e}^{i\Delta\omega t} \\
&\quad - i\sqrt{\frac{\beta}{2}}\left(\sqrt{\bar{N}+\bar{n}}\,\xi_{0+}(t) - \sqrt{\bar{N}-\bar{n}}\,\xi_{0-}(t)\right) \\
\dot{E}_{1x} &= k(1+i\alpha)\left(E_{1x}(g_{1x}-1) + iE_{1y}g_{1xy}\right) + i\gamma_{\mathrm{p}}^{\mathrm{tr}}E_{1x} - (\gamma_{\mathrm{a}} + i\gamma_{\mathrm{p1}})E_{1x} \\
&\quad + \frac{k_{1x}}{\tau_{\mathrm{in}}}\mathrm{e}^{i\Delta\omega t} + \sqrt{\frac{\beta}{2}}\left(\sqrt{\bar{N}+\bar{n}}\,\xi_{1+}(t) + \sqrt{\bar{N}-\bar{n}}\,\xi_{1-}(t)\right) \\
\dot{E}_{1y} &= k(1+i\alpha)\left(E_{1y}(g_{1y}-1) - iE_{1x}g_{1yx}\right) + i\gamma_{\mathrm{p}}^{\mathrm{tr}}E_{1y} + (\gamma_{\mathrm{a}} + i\gamma_{\mathrm{p1}})E_{1y} \\
&\quad + \frac{k_{1y}}{\tau_{\mathrm{in}}}\mathrm{e}^{i\Delta\omega t} - i\sqrt{\frac{\beta}{2}}\left(\sqrt{\bar{N}+\bar{n}}\,\xi_{1+}(t) - \sqrt{\bar{N}-\bar{n}}\,\xi_{1-}(t)\right) \\
\frac{\partial N(r,t)}{\partial t} &= j(t)C(r) + D\nabla_{\perp}^{2}N - \gamma_{\mathrm{e}}\left[N\left(1 + \sum_{i=0,1}\sum_{j=x,y}\left|E_{ij}\right|^{2}\psi_{ij}^{2}(r)\right)\right. \\
&\quad \left. - in\sum_{i=0,1}(E_{ix}E_{iy}^{*} - E_{iy}E_{ix}^{*})\psi_{ix}(r)\psi_{iy}(r)\right]
\end{aligned}$$

$$\frac{\partial n(r,t)}{\partial t} = -\gamma_s n + D\nabla_\perp^2 n - \gamma_e \left[n \sum_{i=0,1} \sum_{j=x,y} \left|E_{ij}\right|^2 \psi_{ij}^2(r) \right.$$
$$\left. -iN \sum_{i=0,1} (E_{ix}E_{iy}^* - E_{iy}E_{ix}^*)\psi_{ix}(r)\psi_{iy}(r) \right] \tag{2}$$

where $N(r,t)$ is the total carrier number and $n(r,t)$ is the difference in the carrier numbers of the two magnetic sublevels. $C(r)$ is the current density such that the total applied current is uniformly distributed across a circular disc contact of $3\,\mu$m radius, equal to the diameter of the waveguide, a, while the prefactor $j(t)$ allows for the generation of current ramps. The normal gain normalized to the threshold gain, $g_{ij}(i=0,1, j=x,y)$, is defined as:

$$g_{ij} = \frac{\int_0^\infty N(r,t)\psi_{ij}^2(r) r\,\mathrm{d}r}{\int_0^\infty \psi_{ij}^2(r) r\,\mathrm{d}r} \tag{3}$$

and $g_{ijk}(i=0,1;\, jk=xy, yx)$ is given by

$$g_{i,jk} = \frac{\int_0^\infty n(r,t)\psi_{ij}(r)\psi_{ik}(r) r\,\mathrm{d}r}{\int_0^\infty \psi_{ij}^2(r) r\,\mathrm{d}r} \tag{4}$$

Note that the modal gains for the x and y polarizations are different due to the different optical mode profiles. However, we neglect the material gain difference since the frequency splitting is very small compared to the width of the gain curve. The injection terms are characterised by the k_{ij} injection strengths, the VCSEL roundtrip time, $\tau_{\mathrm{in}} = 2L/v_g$, and the detuning $\Delta\omega = \omega_{\mathrm{inj}} - \omega_{\mathrm{th}}$, where ω_{inj} is the frequency of the master laser and $\omega_{\mathrm{th}} = (\omega_{0x} + \omega_{0y})/2$, is the central frequency between the two polarizations of the fundamental mode. The injection strength k_{ij} is given by

$$\kappa_{ij} = \left(\frac{1}{\sqrt{R}} - \sqrt{R}\right)\sqrt{\eta_{\mathrm{inj}}}\sqrt{P_{\mathrm{inj},ij}} \tag{5}$$

where R is the output-mirror reflectivity, η_{inj} is the coupling efficiency of the injected light to the optical field in the laser cavity and $P_{\mathrm{inj},ij}$ is the power injected in the j-polarization of the i-transverse mode (van Tartwijk and Lenstra 1995). R and η_{inj} are taken as 0.995 and 1, respectively. Typical values for the region of weak (large) injection are $K_{ij} < 0.01 (K_{ij} \gg 0.1)$ (Annovazzi-Lodi *et al.* 1998).

The rest of parameters that appear in the equations are: the effective cavity length, $L = 1\,\mu$m; the group velocity in the laser cavity, v_g; the field

decay rate, $k = 300\,\mathrm{ns}^{-1}$; the linewidth enhacement factor, $\alpha = 3$; the decay rate for the total carrier population, $\gamma_e = 1\,\mathrm{ns}^{-1}$; the decay rate of the carrier population difference through spin-flip relaxation processes, $\gamma_s = 50\,\mathrm{ns}^{-1}$; the diffusion coefficient, $D = 10\,\mathrm{cm}^2\mathrm{s}^{-1}$; the spontaneous emission coefficient, $\beta = 10^{-5}\,\mathrm{ns}^{-1}$, the strength of the anisotropic gain/losses (dichroism), γ_a; the frequency splitting between the orthogonal polarizations of the $LP_{01}(LP_{11})$ mode, $2\,\gamma_{p0}$ $(2\,\gamma_{p1})$, and the frequency splitting between the two transverse modes with the same polarization, $\gamma_p^{tr}(\gamma_p^{tr}/(2\pi) = 161.4\,\mathrm{GHz})$. The later three parameters are obtained from the calculation of the waveguide modes via the Helmholtz equation. Spontaneous emission noise processes are modeled by the terms $\xi_\pm$ taken as complex Gaussian white noise sources of zero mean and delta-correlated in time. In the noise terms, the carrier distribution is integrated over the active region of radius a:

$$\bar{N} = \frac{\int_0^a N(r,t) r\,\mathrm{d}r}{a^2}, \qquad \bar{n} = \frac{\int_0^a n(r,t) r\,\mathrm{d}r}{a^2} \tag{6}$$

In the following section, we will present the results obtained by integrating numerically the previous set of equations. Time and space integration steps of 0.01 ps and $0.12\,\mu\mathrm{m}$, respectively, have been used. The boundary conditions for the carrier distribution are taken as $N(\infty, t) = 0, n(\infty, t) = 0$. The initial conditions correspond to the stationary solution in the state below threshold corresponding to the initial value of the current ramp $C(r)j(0)$. Further details of the integration method can be found in (Valle 1998b).

3. Injection in single transverse mode vcsels

Polarization properties of single transverse mode VCSELs in the presence of optical injection have been recently analysed in a theoretical (Sciamanna *et al.* 2003b) and in an experimental way (Gatare *et al.* 2004). In both works the polarization dynamics that occurs in the route to polarization switching induced by optical injection was studied. In this problem injection of light from a y-polarized master laser in a VCSEL that emits x-linearly polarised light makes the polarization of the VCSEL to switch to the polarization of the master laser. Previous experimental work only measured the averaged power in the two VCSEL linearly polarized modes (Pan *et al.* 1993). Complex dynamics such as period doubling, quasiperiodicity and chaotic regimes have been found and analysed (Sciamanna 2004). This problem corresponds to a situation where the x-linearly polarized solution of the solitary VCSEL is stable while the y-linearly polarization is unstable. In this section we focus on complementary situations: regions,

where x is unstable and y is stable, both polarizations are stable, and both polarizations are unstable. We assure single-transverse mode operation in the LP_{01} mode by choosing higher losses for the LP_{11} mode in such a way that we get $|E_{1x}|^2 \approx |E_{1y}|^2 \approx 0$. Regions with different stability properties can be found by changing the injected current and the birefringence parameter, γ_{p0}. These situations are illustrated in the stability diagram that appears in the inset of Fig. 1(a). This stability diagram has been obtained without taking into account spatial effects (Martin-Regalado *et al.* 1997b). The x-polarized mode is stable on the right and below the solid line. The y-polarized mode is stable on the left of the dotted line. Just above threshold and for small values of the birefringence there is bistability of the two linearly polarized modes. However, when spatial effects are included in the description the x-polarized mode is always selected at threshold. This selection is due to the modal gain anisotropy induced by the birefringence. Since at low currents the carriers accumulate near the center of the active region, the modal gain of the better confined polarization, the x-mode, is larger than that of the y-mode (see Fig. 1(b)). The polarized Light-Current (L-I) characteristics shown in Fig. 1 has been obtained by increasing linearly the applied current from 0.9 to 2 I_{th} during 200 ns, where I_{th} is the threshold current. The polarization switching ($x \rightarrow y$) observed at around 1.45 I_{th} is due to the combined effect of the AM/FM coupling through the α-factor, VCSEL birefringence and spin-dynamics (Martin-Regalado *et al.* 1997a), since the y-mode has less modal gain when is selected. However, the switching current is slightly higher than the one predicted by the rate equations approach due to spatial effects.

We now analyse the situation in which both polarizations of the fundamental transverse mode are unstable. That situation can be obtained when $I = 2I_{th}$ and $\gamma_{p0} = 12\,\text{ns}^{-1}$ (it corresponds to a $\Delta\nu = 3.8\,\text{GHz}$ splitting between polarizations). We shown in Fig. 2(a) the unstable character of both polarizations by showing their temporal series in the absence of injection. Optical injection of x-polarized light at the central frequency between x and y-LP_{01} modes can be used to stabilise the output of an unstable VCSEL. In Fig. 2(b), we show the temporal series obtained when $k_{0x} = 5 \times 10^{-4}$ and $k_{0y} = 0$: x-polarization is selected in such a way that its intensity displays periodic oscillations. Further increase of k_{0x} selects the x-polarization with a constant value as it can be seen in Fig. 2(c).

Previous dynamical evolutions can be summarised with the help of bifurcation diagrams. In one of those diagrams all the maxima and minima of the power of a polarization that are obtained after a given transient time (that we take as 5 ns) are plotted as a function of the injection strength parameter, in this case k_{0x}. Bifurcation diagrams corresponding to the cases already analysed in Fig. 2 are shown for both polarizations in Fig. 3. Unstable behaviour for both polarizations is obtained

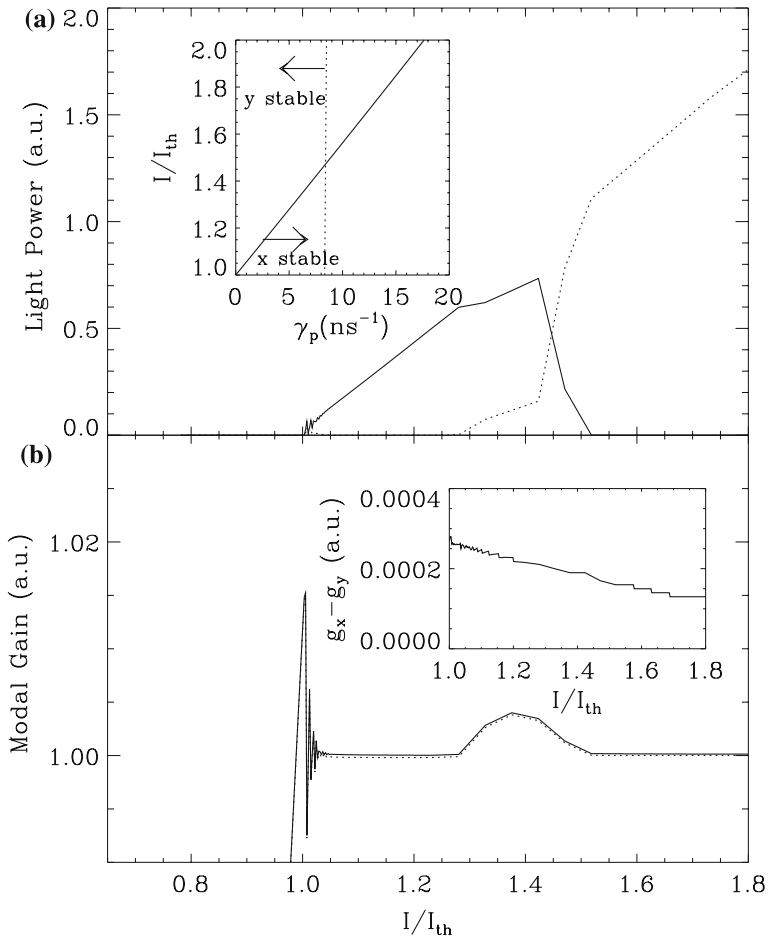

Fig. 1. (a) Light-current characteristics for the linear polarizations of the fundamental transverse mode. The stability diagram appears in the inset. (b) Modal gain versus injection current. Curves related to the $x(y)$-polarizations are plotted with solid (dashed) lines. The inset shows the modal gain difference between the x and y-polarizations. Other parameters in this figure are: $\gamma_{p0} = 6\,\mathrm{ns}^{-1}$ (that corresponds to $\Delta\nu = 1.9\,\mathrm{GHz}$) and $\gamma_a = 0$.

when $k_{0x} < 0.2 \times 10^{-3}$. Selection of x-polarization is achieved when $k_{0x} > 0.2 \times 10^{-3}$. Unstable behaviour occurs only for the x-polarization when $0.2 \times 10^{-3} < k_{0x} < 0.4 \times 10^{-3}$. Larger values of the injection strength lead then to x-polarized periodic evolution until the steady-state evolution is reached when $k_{0x} \sim 0.8 \times 10^{-3}$. This value of the injection strength corresponds to –23 dB of injected power. Steady-state evolution found for $k_{0x} > 0.8 \times 10^{-3}$ corresponds to injection-locked states as it can be seen in the inset of Fig. 3. In that inset the optical spectrum of a VCSEL subject to optical injection when $k_{0x} = 1.2 \times 10^{-3}$ is shown. The optical spectrum

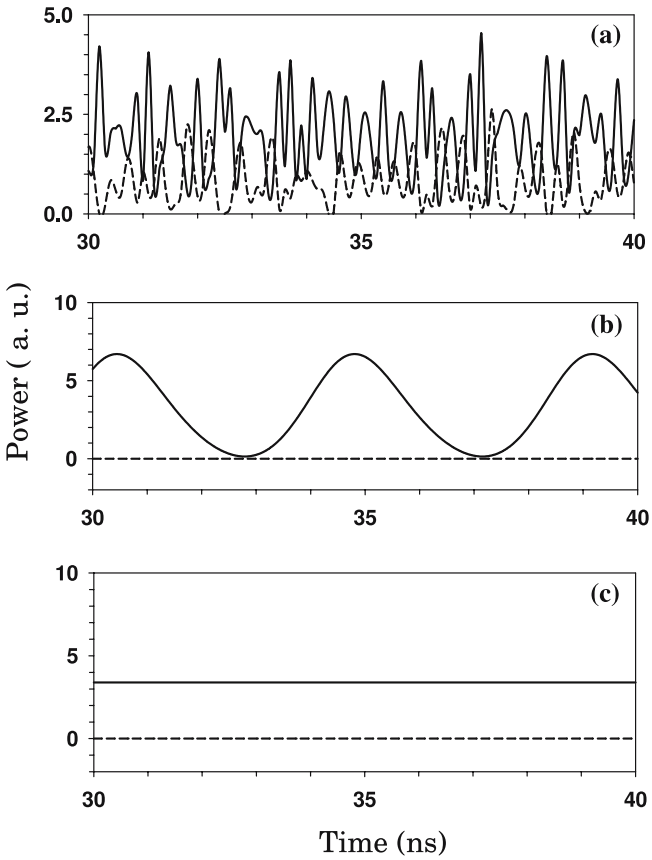

Fig. 2. Power of x (solid) and y (dashed) polarizations of the fundamental transverse mode as a function of time. Parts (a)–(c) correspond to $k_{0x} = 0$, $k_{0x} = 5 \times 10^{-4}$ and $k_{0x} = 1.2 \times 10^{-3}$, respectively. Other parameters in this figure are: $k_{0y} = 0$, $\Delta\omega = 0$, $\gamma_a = 0$ and $n_{\mathrm{core},x} = 3.500041$.

has a maximum at zero frequency showing that the VCSEL locks to the frequency of the external optical signal. Then weak injection of linearly polarized light can lead to stable output power in the injected polarization.

We have also analysed the situation in which x is unstable and y is stable. That region can be reached for instance by choosing $I = 1.6\, I_{\mathrm{th}}$ and $\gamma_{p0} = 6\,\mathrm{ns}^{-1}$. As in the previous analysis x-polarization can be selected by using weak x-polarized optical injection with $\Delta\omega = 0$. A variety of dynamical behaviours again appears as the injection strength is increased. For instance, unstable evolutions for both polarizations can appear ($k_{0x} = 5 \times 10^{-5}$), or selection of a stable x-polarized solution is obtained for values ($k_{0x} > 0.5 \times 10^{-4}$) similar to those obtained when both polarizations are unstable. We finally discuss the situation where both polarizations are stable. That is the case when $I = 1.2 I_{\mathrm{th}}$ and $\gamma_{p0} = 6\,\mathrm{ns}^{-1}$. Again x-polarization

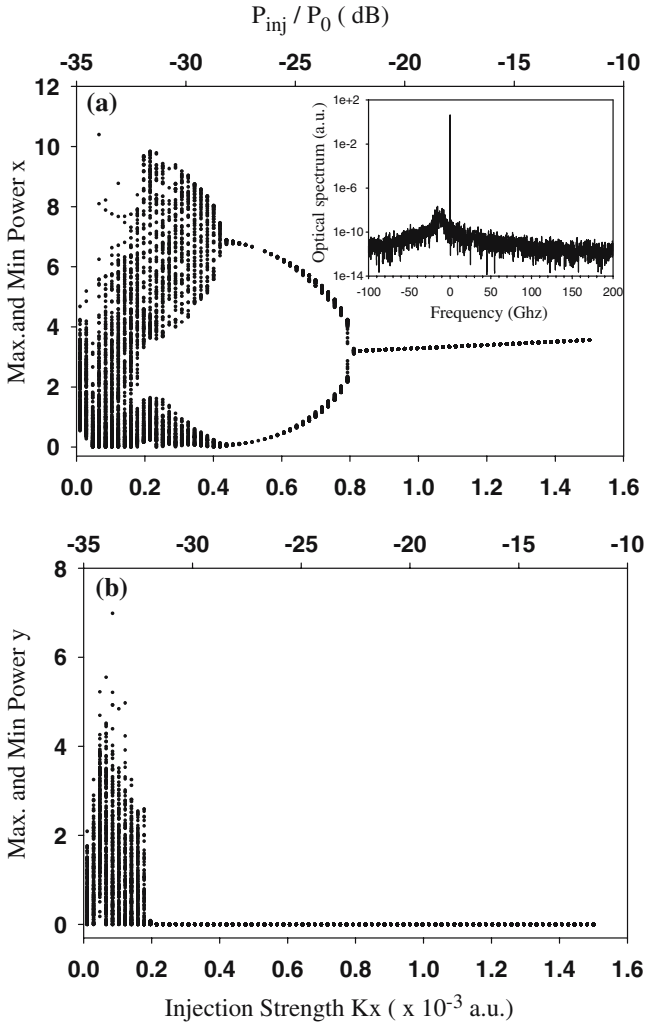

Fig. 3. Bifurcation diagrams for a VCSEL emitting in the LP_{01} mode subject to x-polarized optical injection. Diagrams for the x and y-polarizations are shown in parts (a) and (b), respectively. The inset shows the optical spectrum when $k_{0x} = 1.2 \times 10^{-3}$.

can be selected by using weak x-polarized optical injection with $\Delta\omega = 0$, in such a way that stable x-polarized solution is obtained for values ($k_{0x} > 0.2 \times 10^{-3}$) even lower than those obtained in the previous cases.

4. Injection in multi-transverse mode vcsels

In previous works (Valle *et al.* 1998a) we numerically studied the possible L-I characteristics of multitransverse mode VCSELs in a variety of

situations: different values of dichroism, birefringence, and of the index step were considered to study the combined effect of spin dynamics and spatial hole burning on the polarization behaviour of the device. The L-I curves in this work are obtained by integrating Equation. (2) with an applied current that increase linearly from 0.1 I_{th} to 3.5 I_{th} during the total simulation time (100 ns). The output power was averaged over a time-windows of 1 ns to simulate the bandwidth of the experimental detectors. A typical L-I curve obtained in this way is shown in Fig. 4. For the fundamental transverse mode operation (up to 2.1 I_{th}) the situation is similar to the already discussed in relation with Fig. 1. A polarization switching occurs at 1.4 I_{th} while the modal gain still favours the x-polarized LP_{01} mode. For larger current values, emission occurs in the y-polarized LP_{01} mode up to 2.1 I_{th}. At this current the LP_{11} mode starts lasing orthogonally polarized to the fundamental one in good agreement with previous experimental work (Choquette *et al.* 1995). For even higher currents, a polarization switching is observed but now between the LP_{11} modes with orthogonal polarizations.

We now study the effect of x-linearly polarized optical injection on the previous multimode L-I characteristics. We consider that injection strengths for both x-polarized transverse modes are similar ($k_{0x} = k_{1x} = k_x$) while injection strength in the orthogonal direction is negligible ($k_{0y} = k_{1y} = k_y = 0$). Different situations obtained for different injection strengths of x-polarized light injected with $\Delta\omega = 0$ are shown in Fig. 5. When the injection strength is very weak (Fig. 5(a)) the effect of the optical injection is weak: only a reduction of the current range over which the x-polarized LP_{01} mode dominates is observed. Further increase of k_x leads to unstable

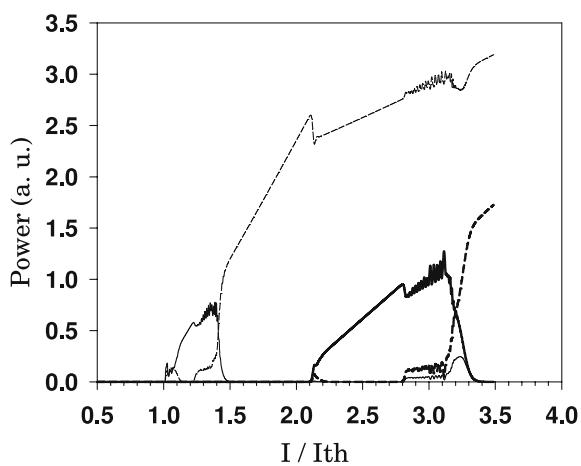

Fig. 4. Light-current characteristics of a multimode VCSEL without optical injection: x-polarized LP_{01} (solid), y-polarized LP_{01} (dashed), x-polarized LP_{11} (solid bold), y-polarized LP_{11} (dashed bold). Other parameters in this figure are $\gamma_{p0} = 6\,ns^{-1}$ (that corresponds to $\Delta\nu = 1.9\,GHz$) and $\gamma_a = 0$.

behaviour as it can be seen in Fig. 5(b). This unstable behaviour can appear for the two polarizations of the fundamental mode ($1.7 < I/I_{th} < 2.1$) or for the two polarizations of both transverse modes ($I/I_{th} > 2.1$). This last situation is shown in Fig. 6(a) where the temporal series of the power of all polarized transverse modes has been plotted when $k_x = 10^{-4}$. Further increase of the injection strength can produce selection of x-polarized light with a regular behaviour in time. That situation is shown in Fig. 5(c) and (d). In both figures the contribution of the LP_{11} mode to the x-polarized light is very small and then selection of the x-polarized LP_{01} mode over a wide range of injection current is achieved. Periodic oscillations that are observed in the L-I curve of Fig. 5(c) are related to the periodic nature of the oscillations of the x-polarized LP_{01} mode for a fixed value of the current. This oscillatory behaviour can be seen in Fig. 6(b) where the temporal series of the power has been plotted when $k_x = 5 \times 10^{-4}$. Selection of x-polarized LP_{01} mode with fixed values of the output power can be obtained by increasing the injection strength as it can be seen in Figs. 5(d) and 6(c). Fig. 5(d) shows that the L-I curve is dominated by the x-polarized LP_{01} mode, while Fig. 6(c) shows that the x-polarized output value of the fundamental mode reaches a constant value for a fixed value of the current. The selection of the x-polarized LP_{01} mode can be obtained by using optical injection independently of the polarization of the transverse modes of the solitary VCSEL. In fact, if we compare Figs. 4 and 5(d) we can see that selection is achieved when the transverse modes of the solitary VCSEL are orthogonal ($2.1 < I/I_{th} < 3.2$) or parallel ($I/I_{th} > 3.2$). The value of the injection strength for which this selection is achieved corresponds, as for the single-mode case, to weak injection: for instance, when $I/I_{th} = 3$, the injected power in Fig. 5(d) is around –17 dB. Previous dynamical evolutions can be summarised with the corresponding bifurcation diagrams. Bifurcation diagrams corresponding to the cases already analysed in Fig. 6 are shown for both polarizations and both transverse modes in Fig. 7. Unstable behaviour for both polarizations is obtained when $k_{0x} < 0.2 \times 10^{-3}$. Selection of x-polarization in the fundamental mode is achieved when $k_{0x} > 0.2 \times 10^{-3}$. Larger values of the injection strength lead then to x-LP_{01} mode periodic evolution until the stable evolution is reached when $k_{0x} \sim 0.9 \times 10^{-3}$.

We now study the effect of injecting x-linearly polarized light with different detunings on the previous multimode L-I characteristics. We choose an injection ($k_x = 1.5 \times 10^{-3}$) in such a way that stable selection of the x-polarized LP_{01} mode over a wide current range is obtained when $\Delta\omega = 0$. Those results were already shown in Fig. 5(d). In Fig. 8, we show the results obtained with different values of the detuning. Better selection than in the zero detuning case is obtained when the detuning is negative, as it can be seen in Fig. 8(a) and (b). This is explained in terms of the

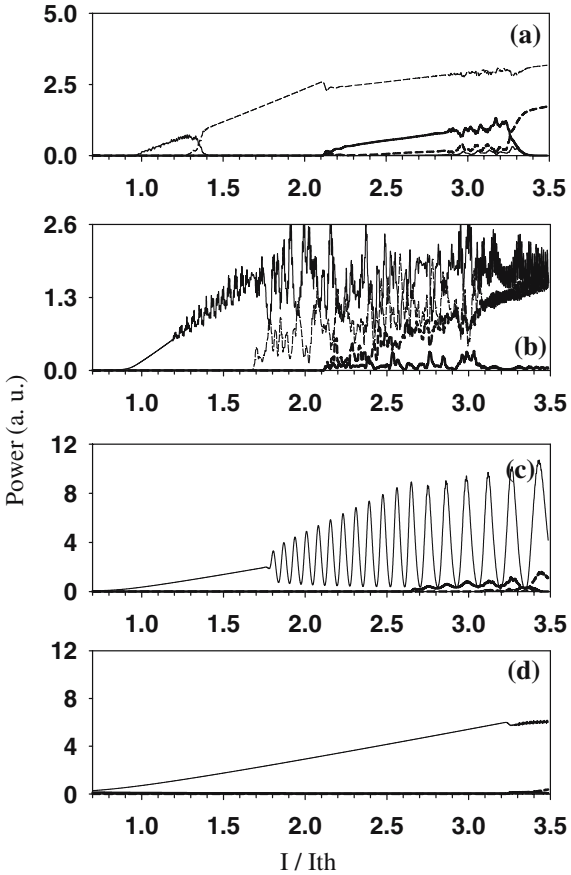

Fig. 5. Light-current characteristics under x-linearly polarized injection for different injection strengths: (a) $k_x = 10^{-5}$, (b) $k_x = 10^{-4}$, (c) $k_x = 5 \times 10^{-4}$, (d) $k_x = 1.5 \times 10^{-3}$. Power of x-polarized LP_{01} (solid), y-polarized LP_{01} (dashed), x-polarized LP_{11} (solid bold) and y-polarized LP_{11} (dashed bold) are shown as a function of the current. Other parameters in this figure are $k_y = 0$, $\Delta\omega = 0$, $\gamma_{p0} = 6\,\mathrm{ns}^{-1}$ and $\gamma_a = 0$.

α-factor induced asymmetry of the stability diagram of a laser diode with optical injection. This asymmetry is such that it is easier to obtain stable outputs when the detuning is negative (van Tartwijk and Lensbra 1995; Law *et al.* 1997). The situation changes when the detuning becomes positive. We show in Fig. 8(c) that for detunings of $\Delta\omega/2\pi = 10\,\mathrm{GHz}$, selection of the x-polarized LP_{01} mode is worse than in previous cases: pure x-polarized LP_{01} light only appears for $I/I_{th} < 2.7$ and fixed values of the power of the x-LP_{01} mode are only obtained if $I/I_{th} < 2.45$. Larger values of the detuning ($\Delta\omega/2\pi = 20\,\mathrm{GHz}$) worsen the previous situation as it can be seen in Fig. 8(d): more irregular power output appears for the x-polarized LP_{01} mode and nonnegligible power of y-LP_{01}, x-LP_{11} and y-LP_{11} modes appear if $I/I_{th} > 2.2$. Selection of a higher order transverse

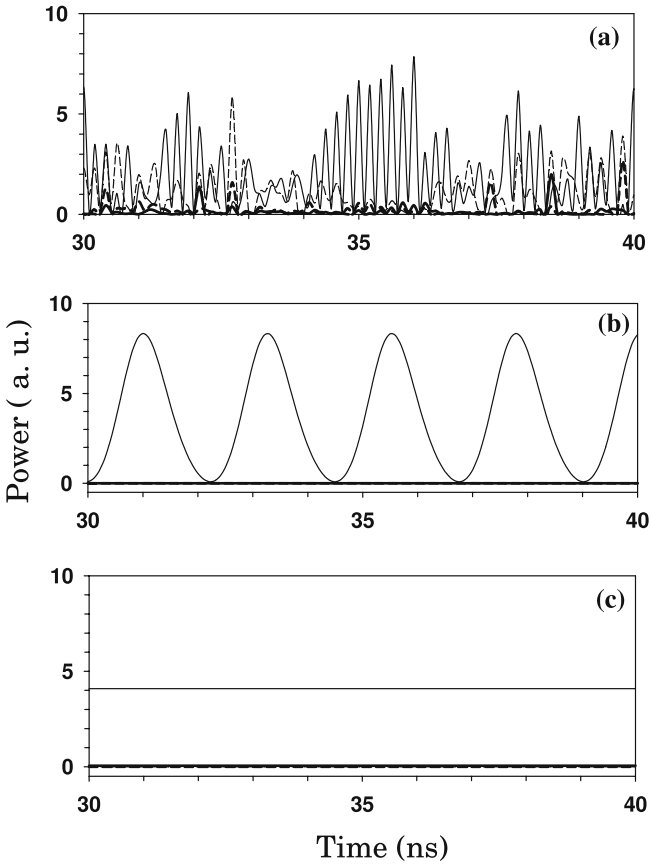

Fig. 6. Power of x-polarized LP_{01} (solid), y-polarized LP_{01} (dashed), x-polarized LP_{11} (solid bold) and y-polarized LP_{11} (dashed bold) modes as a function of time. The VCSEL, biased at $I = 2.2\,I_{th}$, is subject to x-polarized optical injection of strength (a) $k_x = 10^{-4}$, (b) $k_x = 5 \times 10^{-4}$ and (c) $k_x = 1.5 \times 10^{-3}$. Other parameters in this figure are: $ky = 0$, $\Delta\omega = 0$, $\gamma_{p0} = 6\,\text{ns}^{-1}$ and $\gamma_a = 0$.

mode can also be achieved by injecting light at a frequency near its frequency. We have checked it by considering injection of x-polarized light with a detuning that corresponds to the frequency difference between LP_{11} and LP_{01} modes, $\Delta\omega/2\pi = 161.4\,\text{GHz}$. For the specific case in which $I/I_{th} = 2.7$, $k_x = 1.5 \times 10^{-3}$ and $\gamma_{p0} = 6\,\text{ns}^{-1}$ we have obtained that only emission in LP_{11} mode appears, mainly in the x-polarization.

We now focus on the injection of y-linearly polarized light on the multimode L-I characteristics. We now consider that $k_{0y} = k_{1y} = k_y$ while injection strengths in the x-direction are negligible ($k_{0x} = k_{1x} = k_x = 0$). A similar analysis to the already done for x-linearly polarized injection will now be performed. Different L-I curves for different k_y with zero detuning are shown in Fig. 9. When the injection strength is very weak (Fig. 9(a)) the effect

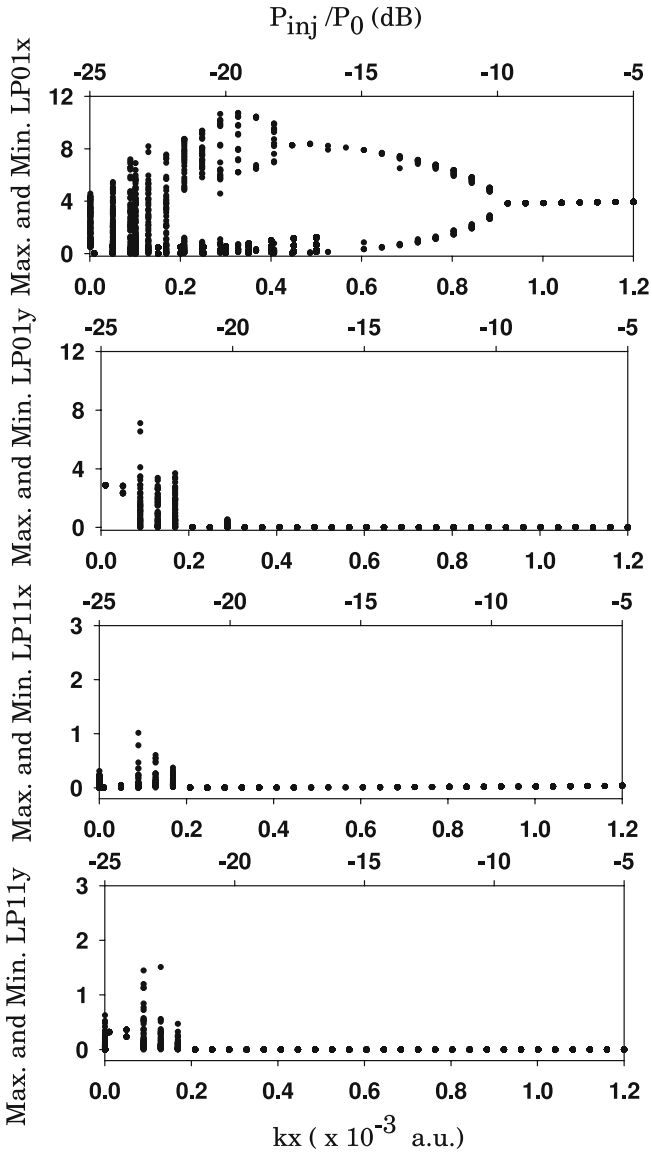

Fig. 7. Bifurcation diagrams for a VCSEL emitting in the LP_{01} and LP_{11} modes subject to x-polarized optical injection. The VCSEL, biased at $I = 2.2\, I_{th}$, is subject to x-polarized optical injection. Other parameters in this figure are: $k_y = 0$, $\Delta\omega = 0$, $\gamma_{p0} = 6\,\mathrm{ns}^{-1}$ and $\gamma_a = 0$.

of the optical injection is the following: emission near threshold of the x-polarized LP_{01} mode dissapears while the rest of the L-I curve remains similar to the one obtained without injection. Fig. 9(b) shows that further increase of k_y leads to slight destabilization of y-LP_{01} mode for $I/I_{th} > 1.7$ while the situation for larger currents with respect to the solitary VCSEL

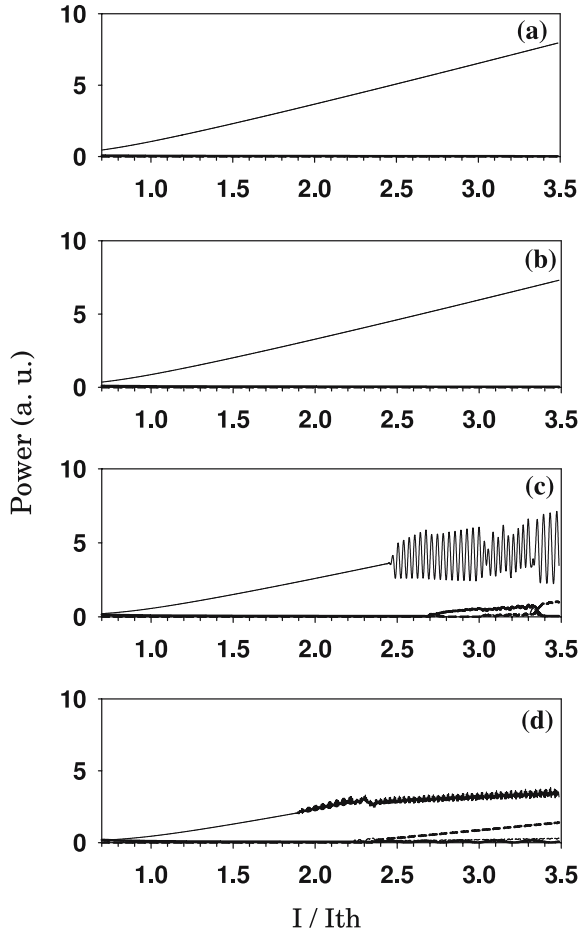

Fig. 8. Light-current characteristics under x-linearly polarized injection for different detunings: (a) $\Delta\omega/2\pi = -20\,\text{GHz}$, (b) $\Delta\omega/2\pi = -10\,\text{GHz}$, (c) $\Delta\omega/2\pi = 10\,\text{GHz}$, (d) $\Delta\omega/2\pi = 20\,\text{GHz}$. Power of x-polarized LP_{01} (solid), y-polarized LP_{01} (dashed), x-polarized LP_{11} (solid bold) and y-polarized LP_{11} (dashed bold) are shown as a function of the current. Other parameters in this figure are $k_x = 1.5 \times 10^{-3}$, $k_y = 0$, $\gamma_{p0} = 6\,\text{ns}^{-1}$ and $\gamma_a = 0$.

does not change too much. Qualitative behaviour of Fig. 9(c) and (d) is similar to the already shown in Fig. 5(c) and (d), respectively, but exchanging x and y. Then selection of the y-polarized LP_{01} mode over a wide range of injection current can be achieved when weak y-polarized light is injected in the VCSEL. Fig. 9(d) shows that the L-I curve is dominated by stable y-polarized LP_{01} mode. Again, the selection of the y-polarized LP_{01} mode can be obtained by using optical injection independently of the polarization of the transverse modes of the solitary VCSEL: selection is achieved when the transverse modes have parallel or orthogonal polarizations.

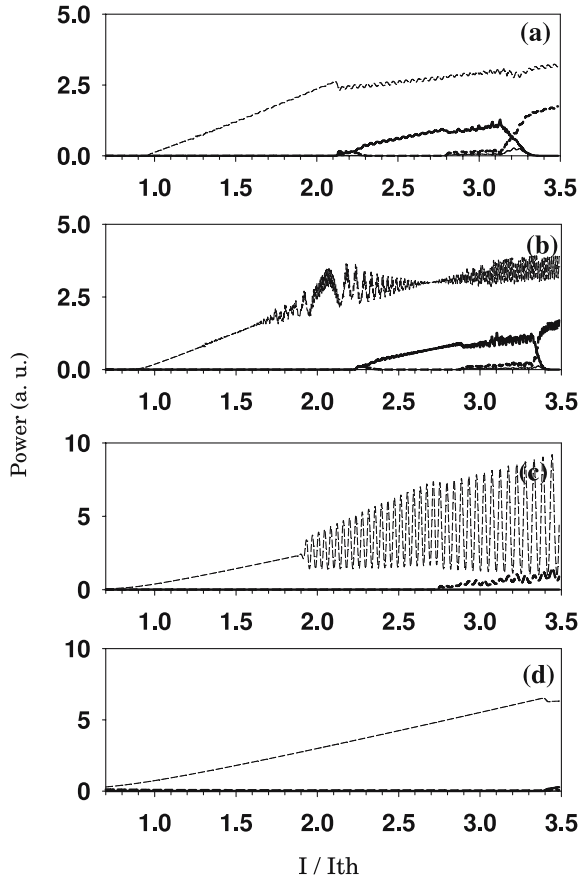

Fig. 9. Light-current characteristics under y-linearly polarized injection for different injection strengths: (a) $k_y = 10^{-5}$, (b) $k_y = 10^{-4}$, (c) $k_y = 5 \times 10^{-4}$, (d) $k_y = 1.5 \times 10^{-3}$. Power of x-polarized LP_{01} (solid), y-polarized LP_{01} (dashed), x-polarized LP_{11} (solid bold) and y-polarized LP_{11} (dashed bold) are shown as a function of the current. Other parameters in this figure are $k_{0x} = 0$, $\Delta\omega = 0$, $\gamma_{p0} = 6\,\mathrm{ns}^{-1}$ and $\gamma_a = 0$.

In Fig. 10, we show the L-I characteristics with injected y-linearly polarized light and considering different values of the detuning. We choose an injection ($k_y = 1.5 \times 10^{-3}$) in such a way that stable selection of the y-polarized LP_{01} mode over a wide current range is obtained when $\Delta\omega = 0$. This result was already shown in Fig. 9(d). As in the previous case, the best selection is obtained when the detuning is negative, as it can be seen in Fig. 10 (a) and (b). In this case the situation also changes when the detuning becomes positive. This behavior is shown in Fig. 10(c) and (d) for positive values of the detunings, $\Delta\omega/2\pi = 10$ and 20 GHz, respectively. An analysis similar to that carried out for the Fig. 8 is valid for this case, with slight modifications in the values of I/I_{th}, as it can be observed in Fig. 10.

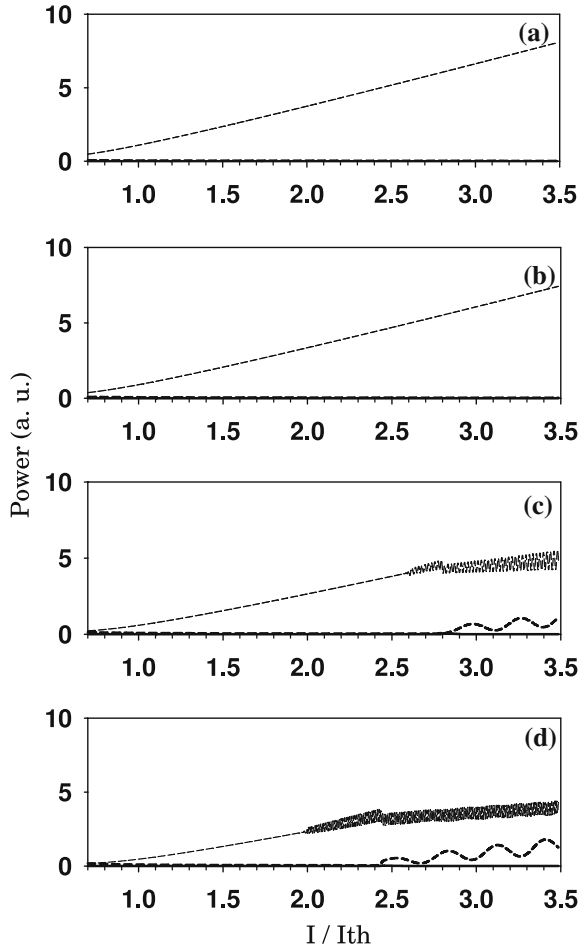

Fig. 10. Light-current characteristics under y-linearly polarized injection for different detunings: (a) $\Delta\omega/2\pi = -20\,\mathrm{GHz}$, (b) $\Delta\omega/2\pi = -10\,\mathrm{GHz}$, (c) $\Delta\omega/2\pi = 10\,\mathrm{GHz}$, (d) $\Delta\omega/2\pi = 20\,\mathrm{GHz}$. Power of x-polarized LP_{01} (solid), y-polarized LP_{01} (dashed), x-polarized LP_{11} (solid bold) and y-polarized LP_{11} (dashed bold) are shown as a function of the current. Other parameters in this figure are $k_y = 1.5 \times 10^{-3}$, $k_x = 0$, $\gamma_{p0} = 6\,\mathrm{ns}^{-1}$ and $\gamma_a = 0$.

We finally discuss on the importance of thermal effects on our results on polarization and transverse mode selection. Light-current characteristics presented in this work are obtained by increasing the current from below to several times threshold during times of the order of 100 ns. For those durations of the current ramps the temperature of the active region remains constant along the ramp (Martin-Regalado *et al.* 1997c). In this way the frequency of the slave VCSEL does not change with the current and the detuning between master and slave laser can be considered as constant along the current ramp, as it has been previously considered. However,

the situation changes if much slower ramps are considered because the frequency of the slave VCSEL becomes dependent of the injected current due to the significative variation of the temperature of the active region of theVCSEL along the current ramp. For typical values of the change of the VCSEL wavelength with the injected current, $\Delta\lambda/\Delta I = 0.3$ nm/mA, (Valle *et al.* 1998c) modal frequencies decrease around 146 GHz when increasing the current from threshold to 3.5 times threshold. This means that if the injected frequency is kept constant along the current ramp and near the frequency of the LP_{01} mode at threshold, at high values of the current (3.5 Ith) the injection frequency would be near the LP_{11} frequency because the frequency difference between LP_{11} and LP_{01} mode is around 161 GHz. Then the selection of the LP_{01} mode would be disfavoured. Summarising, for slow current ramps the mechanism of selection of the LP_{01} mode is effective for all the current range if the frequency of the injection is decreased when increasing the current in the same way in which the slave laser frequency is decreasing. In this way a detuning that is independent of the injected current is obtained and the previous results for faster ramps hold.

5. Summary and discussion

A theoretical analysis of the polarization and transverse modes of VCSELs with external optical injection has been performed. We have shown that, for single-mode operation, weak injection of linearly polarized light can lead to stable output power in the injected polarization. For instance, -23 dB injected power at zero detuning can select the injected polarization when both polarizations are unstable for the solitary VCSEL. We also have shown that, for multitransverse mode operation, weak injection of linearly-polarized light can lead to stable emission of the fundamental transverse mode in the injected polarization over wide current ranges. For instance, injection of around –17 dB selects the fundamental mode in the injected polarization for currents as large as 3.5 I_{th} when the detuning is negative or zero. This current range narrows as the detuning becomes positive. For instance, when the detuning is 10 GHz the fundamental mode in the injected polarization is only selected for currents smaller than 2.5 I_{th}. We have shown that the previous selection can occur when the transverse modes have parallel or orthogonal polarizations. We finally discuss the dependence of the previous results on several parameters of the system. One of the most relevant parameters is the index step of the waveguide of the VCSEL. Larger values of that index step cause that more transverse modes can be supported by the waveguide. These modes are better confined, spatial overlap of the modes with the carrier profile, and hence

modal gains, change. Then the obtained L-I curve appreciably differs to the obtained with a smaller index step. Preliminary results indicate that when the index step increase to 0.01 and competence between polarized LP_{01} and LP_{11} is considered the selection of the fundamental transverse mode in the injected polarization is not as efficient as in the case studied in this work (0.005 index step). Also the refractive index anisotropy or the spin-flip relaxation rate are another parameters which values have an important influence on the L-I curve and therefore on the optical injection induced selection of a linearly-polarized fundamental mode. We have recently analysed the limit case of very small refractive index anisotropy and very large spin-flip relaxation rate in a multitransverse mode VCSEL (Casal *et al.* 2005 unpublished). Our results indicate that selection of a linearly polarized LP_{01} mode can be obtained by weak optical injection independently of the polarization of the LP_{11} mode. Future work will be devoted to understand better the impact of those parameters on the selection of a linearly polarized transverse mode by using external optical injection. This selection process will be better understood by using two-dimensional plots of the intensity of the different polarizations and modes as a function of the injection strength and detuning.

Acknowledgements

This work was supported by CICYT (Spain) under Project TIC2002-04255-C04-01. M.S.T was supported in part by a grant from CONICET (Argentina) PIP 2779 and FONCyT Grant 3/9598. The authors acknowledge the reviewers of the paper for their interesting and useful comments.

References

Annovazzi-Lodi, V., A. Scire, M. Sorel and S. Donati. *IEEE J. Quantum Electron.* **34** 2350, 1998.

Balle, S., E. Tolkachova, M. San Miguel, J.R. Tredicce, J. Martín-Regalado and A. Gahl. *Opt. Lett.* **24** 1121, 1999.

Bandoyopadhyay, S., Y. Hong, P.S. Spencer and K.A. Shore. *J. Lightwave Technol.* **21** 2395, 2003.

Chang-Hasnain, C.J., J.P. Harbison, G. Hasnain, A.C. von Lehmen, L.T. Florez and N.G. Stoffel. *IEEE J. Quantum Electron.* **27** 1402, 1991.

Chang, C.H., L. Chrostowski and C.J. Chang-Hasnain. *IEEE J. Select. Topics Quantum Electron.* **9** 1386, 2003.

Choquette, K. D., R.P. Schneider, K.L. Lear and R.E. Leibenguth, *IEEE J. Select. Topics Quantum Electron.* **1** 661, 1995.

Gatare, I., M. Triginer, H. Thienpont, K. Panajotov and M. Sciamanna. *Proc. Symp. IEEE/LEOS Benelux Chapter* **143**, 2004.

Hong, Y., P.S. Spencer, P. Rees and K.A. Shore. *IEEE J. Quantum Electron.* **38** 274, 2002.

Hong, Y., P.S. Spencer, S. Bandyopadhyay, P. Rees and K.A. Shore. *Optics Comm.* **216** 185, 2003.

Lang, R. *IEEE J. Quantum Electron.* **18** 976, 1982.

Law, J.Y., G.H.M. van Tartwijk and G.P. Agrawal. *Quantum Semiclass. Opt.* **9** 737, 1997.

Li, H., T.L. Lucas, J.G. McInerney, M.W. Wright and R.A. Morgan. *IEEE J. Quantum Electron*. **32** 227, 1996.

Martín-Regalado, J.M., Balle, S., San Miguel M., Valle, A. and Pesquera L. *Quantum Semiclass. Opt*. **9** 713, 1997a.

Martín-Regalado, J.M., F. Prati, M. San Miguel and N.B. Abraham. *IEEE J. Quantum Electron*. **33** 765, 1997b.

Martín-Regalado, J., Chilla, J.L.A., Rocca, J.J., Brusenbach, P. *Appl. Phys. Lett*. **70** 3350, 1997c.

Mulet, J. and S. Balle. *Phys. Rev. A* **66**(5) 053802, 2003.

Onishi, Y., F. Koyama, N. Nishiyama, C. Caneau and C.E. Zah. *Appl. Phys. Lett*. **84**(17) 3247, 2004a.

Onishi, Y., N. Nishiyama, C. Caneau, F. Koyama and C.E. Zah. *IEEE Photon. Technol. Lett*. **16** 1236, 2004b.

Pan, Z. G., S. Jiang, M. Dagenais, R.A. Morgan, K. Kojima, M.T. Asom and R.E. Leibenguth. *Appl. Phys. Lett*. **63** 2999, 1993.

Panajotov, K., B. Ryvkin, J. Danckaert, M. Peeters, H. Thienpont and I. Veretennicoff. *IEEE Photon. Technol. Lett*. **10** 6, 1998.

Ryvkin, B., K. Panajotov, A. Georgievski, J. Danckaert, M. Peeters, G. Verschaffelt, H. Thienpont and I. Veretennicoff. *J. Opt. Soc. Am. B* **16** 2106, 1999.

San Miguel, M., Q. Feng and J.V. Moloney. *Phys. Rev. A* **52** 1728, 1995.

Sciamanna, M., A. Valle, K. Panajotov, P. Megret and M. Blondel. *Phys. Rev. E* **68** 016207, 2003a.

Sciamanna, M., K. Panajotov, G. Monticelli, A. Tabaka, H. Thienpont and I. Veretennicoff. *CLEO/IQEC*, EA-11438, 2003b.

Sciamanna, M. PhD Thesis, Fac. Polytechnique de Mons, Belgium, 2004.

Torre, M.S., C. Masoller and K.A. Shore. *IEEE J. Quantum Electron*. **40** 25, 2004.

Vakhshoori, D., J.D. Wynn, G.J. Zydzik, M. Asom, K. Kojima, R.E. Leibenguth and R.A. Morgan. *Appl. Phys. Lett*. **62**(13) 1448, 1993.

Valle, A., J. Sarma and K.A. Shore. *IEEE J. Quantum Electron*. **31** 1423, 1995.

Valle, A., K.A. Shore and L. Pesquera. *J. Lightwave Technol*. **14** 2062, 1996.

Valle, A., L. Pesquera and K.A. Shore. *IEEE Photon. Technol. Lett*. **9** 557, 1997.

Valle, A., J.M. Martín-Regalado, L. Pesquera, S. Balle and M. San Miguel. *Proc SPIE* **3283** 280, 1998a.

Valle, A. *IEEE J. Quantum Electron*. **34** 1924, 1998b.

Valle, A., Pesquera, L., Shore, K.A. *IEEE Photon. Technol. Lett*. **10** 639, 1998c.

Valle, A., L. Pesquera, S.I. Turovets and J.M. Lopez. *Opt. Comm*. **208** 173, 2002.

Van Tartwijk, G.H.M. and D. Lenstra. *Quantum Semiclass. Opt*. **7** 87, 1995.

Yu, S.F., P. Shum, and J.Q.N. Ngo. *Opt. Comm*. **200** 143, 2001.